



## The prediction of drug metabolism using scaffold-mediated enhancement of the induced cytochrome P450 activities in fibroblasts by hepatic transcriptional regulators

Tsai-Shin Chiang<sup>a,1,2</sup>, Kai-Chiang Yang<sup>b,1,3</sup>, Shu-Kai Zheng<sup>c</sup>, Ling-Ling Chiou<sup>d</sup>, Wen-Ming Hsu<sup>e</sup>, Feng-Huei Lin<sup>f,4</sup>, Guan-Tarn Huang<sup>c,\*\*</sup>, Hsuan-Shu Lee<sup>a,c,g,h,\*</sup>

<sup>a</sup> Institute of Biotechnology, College of Bioresources and Agriculture, National Taiwan University, 4F, No. 81, Chang-Xing St., Taipei 106, Taiwan

<sup>b</sup> School of Dentistry, College of Oral Medicine, Taipei Medical University, No. 250, Wu-Hsing St., Taipei 11031, Taiwan

<sup>c</sup> Department of Internal Medicine, National Taiwan University Hospital and National Taiwan University, No. 1, Jen Ai Road, Section 1, Taipei 10051, Taiwan

<sup>d</sup> Liver Disease Prevention and Treatment Research Foundation, No. 1, Jen Ai Road, Section 1, Taipei 10051, Taiwan

<sup>e</sup> Department of Surgery, National Taiwan University Hospital, No. 1, Jen Ai Road, Section 1, Taipei 10051, Taiwan

<sup>f</sup> Institute of Biomedical Engineering, College of Engineering and College of Medicine, National Taiwan University, No. 1, Section 1, Jen Ai Road, Taipei 10051, Taiwan

<sup>g</sup> Agricultural Biotechnology Research Center, Academia Sinica, Taipei, Taiwan

<sup>h</sup> Research Center for Developmental Biology and Regenerative Medicine, National Taiwan University, Taipei, Taiwan

### ARTICLE INFO

#### Article history:

Received 27 March 2012

Accepted 4 April 2012

Available online 26 April 2012

#### Keywords:

Human dermal fibroblast

Cytochrome P450

Transcriptional regulator

Scaffold

Drug metabolism

### ABSTRACT

A reliable, reproducible, and convenient *in vitro* platform for drug metabolism determination and toxicity prediction is of tremendous value but still lacking. In the present study, a collection of 24 hepatic transcription factors and nuclear receptors in different combinations were surveyed, and 10 among them were finally selected to induce the expression and enzyme activities of cytochrome P450 (CYP) 3A4, 1B1, and 2C9 in human dermal fibroblasts (HDFs). The expression and activities of these CYPs in the induced HDFs were higher than those in commonly used hepatoma cell lines. High CYP expression and activities could be further enhanced by culturing the induced HDFs either as spheroids or into several kinds of scaffolds, particularly the tri-copolymer scaffold composed of gelatin, chondroitin and hyaluronan. More strikingly, there showed a synergistic effect of seeding and culturing the spheroids into the tri-copolymer scaffold. Scanning electron microscopy and confocal microscopy disclosed well accommodation of these spheroids inside the scaffolds and displayed a high survival rate. Moreover, the spheroid/scaffold constructs could metabolize an anti-hypertension drug nifedipine into oxidized nifedipine, showing their applicability in studying drug metabolism. This study presents a strategy to induce the expression and enzyme activities of critical CYPs in HDFs, and may have potential to establish an *in vitro* platform to study drug metabolism and to predict the possible human risk of drug toxicity.

© 2012 Elsevier Ltd. All rights reserved.

### 1. Introduction

The concern of drug safety is a serious issue for the public and health organizations, while a critical challenge to the pharmaceutical industry. Many drugs have been withdrawn from the market, and over 40% of marketing candidate drugs terminated due to unexpected toxic effects [1,2]. This outcome represented a severe harm to the patients and a huge loss of money from the industry. For decades, drug-induced hepatotoxicity accounted for around 30% of drug withdrawals from the market [1,3,4]. Apparently the traditionally used toxicity assays based on animal studies have failed to recognize the potential human risk of hepatotoxicity of these compounds during their development. Animal tests are expensive and of low throughput, yet frequently of questionable

\* Corresponding author. Institute of Biotechnology, College of Bioresources and Agriculture, National Taiwan University, 4F, No. 81, Chang-Xing St., Taipei 106, Taiwan. Tel.: +886 2 2312 3456x65194; fax: +886 2 3366 6001.

\*\* Corresponding author. Tel.: +886 2 2312 3456x65015; fax: +886 2 23819723.

E-mail addresses: [d97642003@ntu.edu.tw](mailto:d97642003@ntu.edu.tw) (T.-S. Chiang), [pumpkin@tmu.edu.tw](mailto:pumpkin@tmu.edu.tw) (K.-C. Yang), [b90205212@ntu.edu.tw](mailto:b90205212@ntu.edu.tw) (S.-K. Zheng), [hslee@ntu.edu.tw](mailto:hslee@ntu.edu.tw) (L.-L. Chiou), [wmhsu@ntu.edu.tw](mailto:wmhsu@ntu.edu.tw) (W.-M. Hsu), [double@ntu.edu.tw](mailto:double@ntu.edu.tw) (F.-H. Lin), [gthuang@ntu.edu.tw](mailto:gthuang@ntu.edu.tw) (G.-T. Huang), [benlee@ntu.edu.tw](mailto:benlee@ntu.edu.tw) (H.-S. Lee).

<sup>1</sup> These authors contributed equally to this work.

<sup>2</sup> Tel.: +886 2 3366 6008; fax: +886 2 3366 6001.

<sup>3</sup> Tel.: +886 2 2736 1661x5125; fax: +886 2 2736 2295.

<sup>4</sup> Tel.: +886 2 2312 3456x81456; fax: +886 2 2394 0049.

relevance to predicting human risks because of inter-species differences [5]. Therefore, several government authorities have proposed an urgent requirement for moving away from traditional animal toxicology tests to new approaches based on well-designed *in vitro* platforms using human cells or tissues [6].

For *in vitro* evaluations of hepatotoxic risks, human liver slices, liver microsomes, hepatoma cell lines, and primary hepatocytes are used frequently [7,8]. However, liver slices are viable for ~1 day only, and human liver microsomes lack dynamic gene expression profiles. In spite of human hepatoma cell lines are relatively accessible, the expression levels and activities of drug-metabolizing enzymes have been shown extremely low, comparing to primary hepatocytes, beyond the range able to demonstrate certain drug-induced hepatotoxicity [7,9]. Although human hepatocytes are the most ideal cells for predicting drug toxicity, the cell source is quite limited and the activities of phase I cytochrome P450 (CYP) enzymes decline rapidly under traditional culture conditions [10,11]. Therefore, it is of critical importance to develop an *in vitro* platform with appropriate CYPs activities for risk assessment of drug-induced hepatotoxicity.

CYPs located in mitochondria and endoplasmic reticulum are the major phase I enzymes present in the liver for metabolizing endogenous and exogenous chemicals including drugs [12]. CYP1, CYP2, and CYP3 family members are relevant to drug biotransformation in human liver [13]. More than half of clinical drugs and xenobiotics in use today are metabolized by CYP3A4 and CYP2C9 [12,14]. However, their expression levels are usually very low in cells of currently used prediction systems. Expressions of these enzymes are coordinately regulated by several hepatocyte-enriched transcription factors and nuclear receptors at transcriptional level in the liver [13,15–18]. Besides, cell–cell communication and microenvironment stimulation also help the cultured hepatocytes to maintain their functions of these CYP enzymes [19]. Three dimensional (3D) culture systems have been shown to improve cell–cell and cell–matrix interactions and hence have positive effects to preserve structural polarity and maintain cellular functions [20–22]. Over the last decade, many studies have demonstrated that higher levels of liver-specific functions of hepatocytes could be maintained better in 3D than in conventional monolayer culture [23–25]. To this end, several 3D culturing methods such as spheroid formation, collagen sandwich gel culture, microencapsulation of cells, and seeding of cells into natural or synthetic biodegradable scaffolds have been commonly used for culturing hepatocytes and hepatic cell lines [26–28].

In this study, we established a strategy to induce expression and activities of CYP3A4, CYP1B1 and CYP2C9 in human dermal fibroblasts (HDFs) by delivery of several hepatocyte-enriched transcription factors and nuclear receptors using a lentivirus system. Next, the CYP activities were further augmented by forming the cells into spheroids and by sequential spheroid formation and scaffold cultivation in gelatin–chondroitin–hyaluronan (GCH) tri-copolymer scaffolds [29].

## 2. Materials and methods

### 2.1. Cell culture

Retrieval and use of human tissue and cells were approved by the Research Ethical Committee at NTUH (201201007RID). HDFs were primarily cultured from human foreskin tissues obtained by circumcision. The human embryonic kidney 293T cells and human hepatoma cell lines HepG2 and Hep3B were obtained from American Type Culture Collection (ATCC, Manassas, VA, USA). Another human hepatoma cell line HuH-7 was from Japanese Collection of Research Bioresources (JCRB, Ibaraki, Osaka, Japan). All the cells were cultured in Dulbecco's Modified Eagle's Medium (DMEM, GIBCO-BRL, Scotland, UK) supplemented with 10% fetal bovine serum (FBS) at 37 °C under an atmosphere containing 5% CO<sub>2</sub>. HDFs between 7 and 10 passages were used in this study. To be formed into spheroids, HDFs were

cultured on HydroCell dishes (Thermo Scientific, Tokyo, Japan) whose surface was covalently immobilized with super hydrophilic polymer to prevent cell attachment.

### 2.2. Plasmid construction and production of recombinant lentiviruses

The coding sequence of the complementary DNAs (cDNAs) of 24 human hepatocyte-enriched transcription factors and nuclear receptors were either cloned by reverse transcription-polymerase chain reaction (RT-PCR) from human hepatoma cell lines or directly synthesized. These cDNAs were subcloned into pCDH cDNA Expression Lentivector (System Biosciences, Mountain View, CA, USA). The expression of the inserts would be driven by a CMV promoter while a reporter copGFP be driven by a separate promoter EF1. The cloned genes include hepatocyte nuclear factor (*Hnf1a*, *Hnf1b*, *Hnf3a*, *Hnf3b*, *Hnf4a*, *Hnf6*, CCAAT-enhancer binding protein alpha (*C/ebpα*) and beta (*C/ebpβ*), GATA binding protein 6 (*Gata6*), V-rel reticuloendotheliosis viral oncogene homolog A (*Rel-a*), SRY-box (*Sox17*), H2.0-like homeobox-1 (*Hlx-1*), X-box-binding protein 1 (*Xbp-1*), aryl hydrocarbon receptor (*AhR*), pregnane X receptor (*Pxr*), retinoid X receptor (*Rxr*), liver X receptor (*Lxr*), farnesoid X receptor (*Fxr*), constitutive androstane receptor (*Car*), nuclear receptor subfamily 2, group F, member 2 (*Nr2f2*), nuclear receptor subfamily 5, group A, member 2 (*Nr5a2*), aryl hydrocarbon receptor nuclear translocator (*Arnt*), glucocorticoid receptor (*Gr*), and interleukin 6 signal transducer (*Gp130r*). To produce recombinant lentiviruses, 293T cells ( $1 \times 10^6$  cells) were seeded into 10-cm dishes and co-transfected with respective recombinant expression lentivectors in combination with envelop plasmid pMD2.G and packaging plasmid pSPAX2 (deposited to Addgene, Cambridge, MA, by Dr. Didier Trono, School of Life Sciences and Frontiers in Genetics Program, Lausanne, Switzerland) using jetPEI™ transfection reagent (Polyplus-Transfection Inc., New York, NY, USA) in accordance with manufacturer's instructions. Supernatants from the transfected 293T cells were collected 2 days after transfection and concentrated by centrifugation ( $4000 \times g$  for 30–60 min at 4 °C) using Amicon Ultra 15 Centrifugal Filter Units (Millipore, Billerica, MA, USA). After filtered through 0.2 μm cellulose acetate filters, virus solutions were stocked in aliquots at –80 °C until used.

### 2.3. Titration of produced lentiviruses by flow cytometry

To determine the transfection unit of the stocked viruses, 293T cells were infected by a series of diluted virus solutions and the percentage of cells positive for the reporter copGFP was determined by flow cytometry using Becton Dickinson FACS Calibur flow cytometry system (BD Biosciences, Mississauga, Canada). The flow cytometric data were analyzed using WinMDI software.

### 2.4. Induction of HDFs by lentivirus infection

Aliquots of  $1 \times 10^4$  HDFs in 0.5 mL of culture medium were seeded in 24-well plates and cultured for 1 day before they were infected by indicated combinations and multiplicity of infection (MOI) of recombinant lentiviruses. The virus-infected cells were maintained for 2 weeks in 24-well plates with a medium change every 2–3 days.

### 2.5. Total RNA isolation, reverse transcription, and quantitative-polymerase chain reaction (Q-PCR)

Total RNAs of the cells were extracted using RNeasy™ C&T reagent (Protech Technologies Inc., Taipei, Taiwan). Reverse transcription was performed by SuperScript III reverse transcriptase (Invitrogen, Carlsbad, CA, USA) with a total volume of 20 μL and the products were used for Q-PCR in which TaqMan system (Applied Biosystems, Foster City, CA, USA) with respective primers/probes was used for chain reaction referring to a house-keeping gene glyceraldehyde-3-phosphate dehydrogenase (GAPDH). The PCR conditions were denaturation at 95 °C for 30 s, annealing at 60 °C for 30 s, and extension at 72 °C for 30 s for up to 40 cycles.

### 2.6. CYP activity assays

Cell-based assays were used to determine cellular activities of CYP3A4, CYP2C9 and CYP1B1 (Promega Corp., Madison, WI, USA). Cells were incubated with substrates (50 μM Luciferin-PFBE for CYP3A4, 100 μM Luciferin-H for CYP2C9, and 100 μM Luciferin-CEE for CYP1B1, respectively) at 37 °C for 3 h with occasional mixing by swirling or inverting. After incubation, an aliquot of 50 μL of medium was transferred from each well to a 96-well opaque white luminometer plate at room temperature, 50 μL of luciferin detection reagent was added into each well to initiate a luminescent reaction for 20 min in the dark, and then luminescence was read using Victor3 luminometer (PerkinElmer, Singapore). Following luminescence determinations, the cells were subjected to extraction of genomic DNA (Geneaid Biotech Ltd., Cleveland, OH, USA). The luminescence reads were normalized to the respectively yielded amount of genomic DNA. In some experiments, CYP inducers rifampicin and omeprazole (Sigma–Aldrich, St. Louis, MO, USA) were added at 25 μM and 100 μM, respectively, to the culture for 72 h before determination of CYP activities according to the protocols of Promega Corporation.

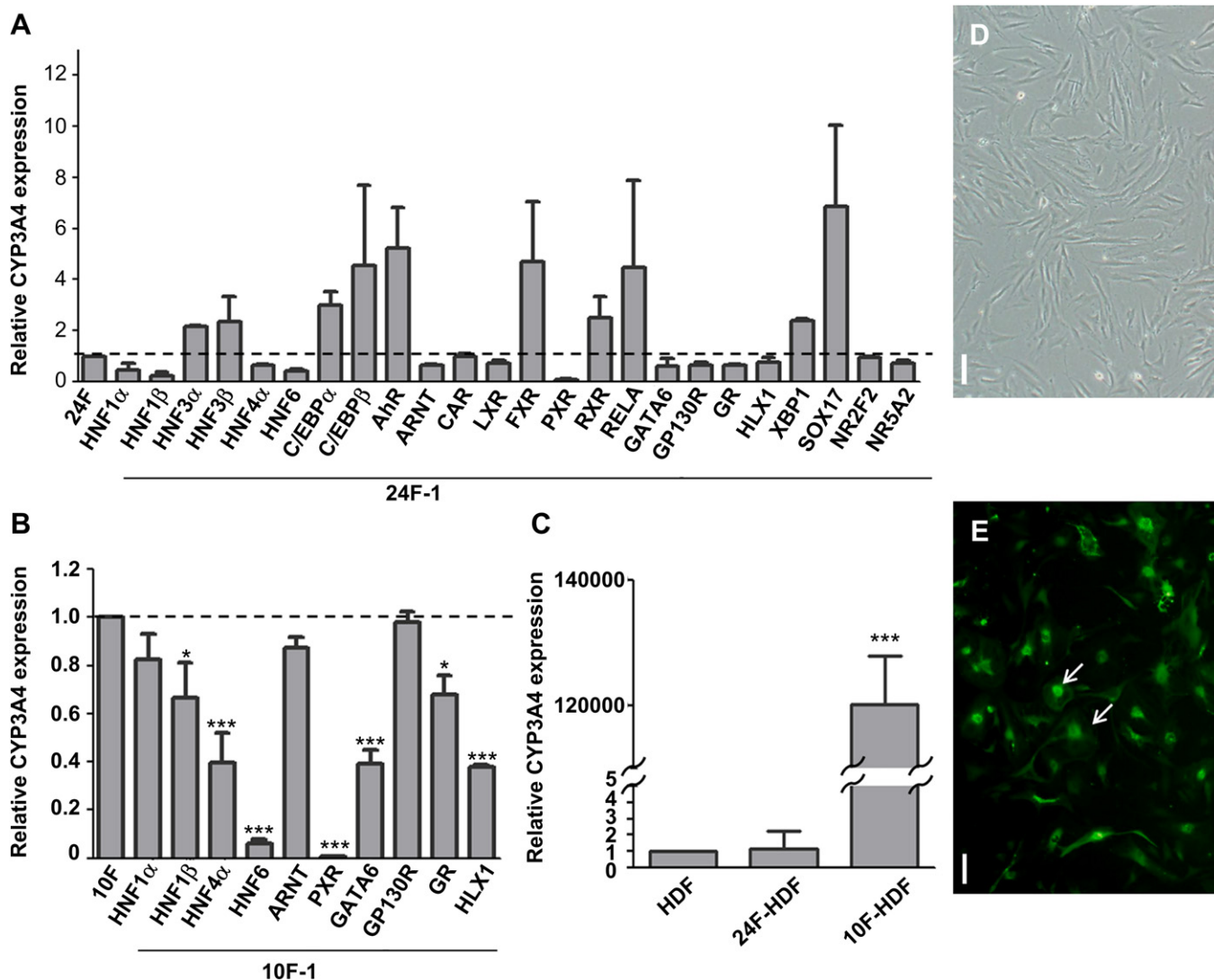


**Fig. 1.** Selection of essential genes optimally inducing CYP3A4 expression in HDFs by Q-PCR. Cells were cultured for 14 days on ordinary cell culture dishes and mRNA levels of CYP3A4 were quantified by Q-PCR. (A) The 1st bar indicates the expression level induced by the pool of 24 factors as the control. The later bars indicate the expression by the 23-factor pools omitting indicated factors, respectively, from the 24 factors. (B) The 1st bar indicates the CYP3A4 expression level by the pool of 10 factors selected from A as the control. The later bars indicate the expression level induced by the 9-factor pools omitting indicated factors, respectively, from the 10 factors. (C) Comparisons of the CYP3A4 expression levels in HDFs without (HDF) and with induction by 24 (24F-HDF) or 10 (10F-HDF) factors. Dotted lines in A and B indicate the control value "1". \* $P < 0.05$ , \*\* $P < 0.01$ , \*\*\* $P < 0.001$ . (D) A representative bright field image of HDFs showing characteristic features of fibroblasts. (E) A representative fluorescent image of HDFs infected with lentiviruses containing 10 factors shows reporter copGFP fluorescence. Note some cells became ovoid (arrows) in contrast to the original elongated shape of fibroblasts. Each scale bar indicates 100  $\mu$ m.

### 2.7. Fabrication of scaffolds

The scaffolds were produced as previously described with some modifications [29,30]. In brief, gelatin (Sigma–Aldrich), chondroitin-6-sulfate (Sigma–Aldrich), sodium hyaluronate (Seikagaku Corp., Tokyo, Japan), type I collagen (BD Biosciences, Bedford, MA, USA) and type IV collagen (Nitta Gelatin Inc., Osaka, Japan) were purchased and keratin was homemade from human hair bleached by peracetic acid and protein extracted in 100 mM Tris. Respective materials or mixture of gelatin, chondroitin and hyaluronan (for producing GCH tri-copolymer scaffold) were cross-linked in 0.1% glutaraldehyde (Sigma–Aldrich), frozen overnight, lyophilized, cross-linked again by glutaraldehyde, treated by 0.1 M glycine to remove residual free glutaraldehyde, and at last lyophilized again. The fabricated gelatin, GCH tri-copolymer, type I and type IV collagen and keratin scaffolds were now ready for use. These scaffolds were cut into  $3 \times 3 \times 3$  mm cubes for cell seeding. The pore size of scaffolds thus formed was in the range between 150 and 200  $\mu$ m and the porosity around 75–80%.

### 2.8. Seeding cells into scaffolds

The scaffold cubes were sterilized with 75% ethanol and then washed twice with phosphate-buffered saline (PBS) to remove the residual ethanol before cell seeding. The cells in single cell suspension or in spheroids were suspended in medium and then seeded into scaffolds by gravity. The scaffolds were placed in a culture dish for

30 min for cell adhesion, and then cultured in 6-well plates for 7 days before assessment of gene expression and enzyme activities. The medium was changed every other day.

### 2.9. Preparation of scaffold for scanning electron microscopy

After cultured for 7 days, the scaffolds containing cells were dehydrated by treatment with a series of graded ethanol solutions and followed by critical point drying. They were subsequently coated with gold for imaging by scanning electron microscopy (SEM, S-800 Field emission scanning electron microscope, Hitachi, Tokyo, Japan).

### 2.10. Live/dead assay of cells cultured as spheroids

Cell viability in the spheroids was determined by LIVE/DEAD<sup>®</sup> Violet Viability/Vitality Kit (Invitrogen). Live cells were stained blue by calcein violet AM (ex/em = 400/452  $\pm$  5 nm), dead cells stained red by Aqua-fluorescent reactive dye (ex/em = 400/526  $\pm$  5 nm) and total cell nuclei were stained blue by Hoechst 34580 (ex/em = 392/440  $\pm$  5 nm). The stained spheroids were imaged by a confocal microscope (TCS SP5 II, Leica, Buffalo Grove, IL, USA).

From the biggest plane of respective spheroids, dead cell number was divided by total nuclei number to yield a "dead cell rate".

### 2.11. CYP3A4 activity assay by measuring metabolized nifedipine (NIF)

A stock solution of oxidized nifedipine (ONIF, Sigma) at 100 nmol/mL was prepared with acetonitrile (ACN)–water solution (80:20, v/v). A standard calibration curve of ONIF was constructed with concentrations of 0.001, 0.01, 0.05, 0.1, 0.5, 1, and 10 nmol/mL.

To measure cellular activities of CYP3A4 that metabolize NIF into ONIF, cells were incubated in the medium containing 10 µg/mL NIF for 24 h. An aliquot of 500 µL of the medium was centrifuged at 12,000× *g* for 10 min and then the supernatant was mixed with the same volume of 80% ACN before measurement of ONIF by high performance liquid chromatography–electrospray tandem mass spectrometry (HPLC–ESI–MS/MS). A ThermoFinnigan LXQ Advantage ion trap mass spectrometer (San Jose, California, USA) coupled with a ThermoFinnigan Surveyor liquid chromatography system was employed for the measuring. The extracts were injected into a reversed phase column (Phenomenex Kinetex 2.6 µ, C18, 100A, 150 × 2.10 mm) at a flow rate of 0.2 mL/min. Eluted peaks at 269 nm for ONIF were monitored by a photodiode array detector. The area under each peak was recorded and interpolated using the standard line to indicate moles of ONIF, and then normalized by respective amount of genomic DNA.

### 2.12. Statistics

Data are presented as mean ± SE. A one-way ANOVA analysis with a post-hoc Dunnett's multiple comparison tests was used to analyze the differences between subgroups. Differences were considered statistically significant at *P* values less than 0.05. For all statistics, data from triplicate or 3 independent experiments were used.

## 3. Results

### 3.1. Selection of 10 from 24 factors optimally inducing CYP3A4 expression in HDFs

Because CYP3A4 is the most abundant and important among liver CYPs in metabolizing exogenous xenobiotics and drugs, we tried to select a combination among the 24 cloned hepatocyte-

specific factors to optimally express CYP3A4 in HDFs. The recombinant lentiviruses (each at 75 MOI) were used to infect HDFs for 2 weeks in ordinary culture dishes coated with polystyrene. In addition to all the prepared 24 factors, we also infected the cells using virus pools omitting respective one from the 24 factors. The Q-PCR analysis (Fig. 1A) showed omission of some factors increased CYP3A4 expression, while omission of others reduced the expression. The former factors were considered having inhibitory effects to CYP3A4 expression in HDFs and the latter ones having up-regulating effects. We then picked up 10 from the latter factors for further studies. They included HNF1α, HNF1β, HNF4α, HNF6, ARNT, PXR, GATA6, GP130R, GR and HLX1. Elimination of anyone from the 10 did not increase the expression of CYP3A4 (Fig. 1B). Compared to the original HDFs, transduction of 24 factors (24F-HDFs) only increased the expression to 1.16-fold, while transduction of the selected 10 factors (10F-HDFs) dramatically increased it to 10<sup>5</sup>-fold (Fig. 1C). Compared to the original elongated HDFs, the 10F-HDFs became more ovoid in shape and of course showed green fluorescence of the reporter copGFP (Fig. 1D).

### 3.2. Comparing 10F-HDFs with human hepatoma cell lines regarding their gene expression and enzyme activities of CYP3A4, CYP1B1 and CYP2C9

As alternatives to human hepatocytes whose sources were limited, human hepatoma cell lines were frequently used to determine drug metabolism though their drug-metabolizing activities were much lower than hepatocytes [7,9]. Here we compared our 10F-HDFs with human hepatoma cell line Hep3B, HepG2 and HuH-7 regarding their expression and functional

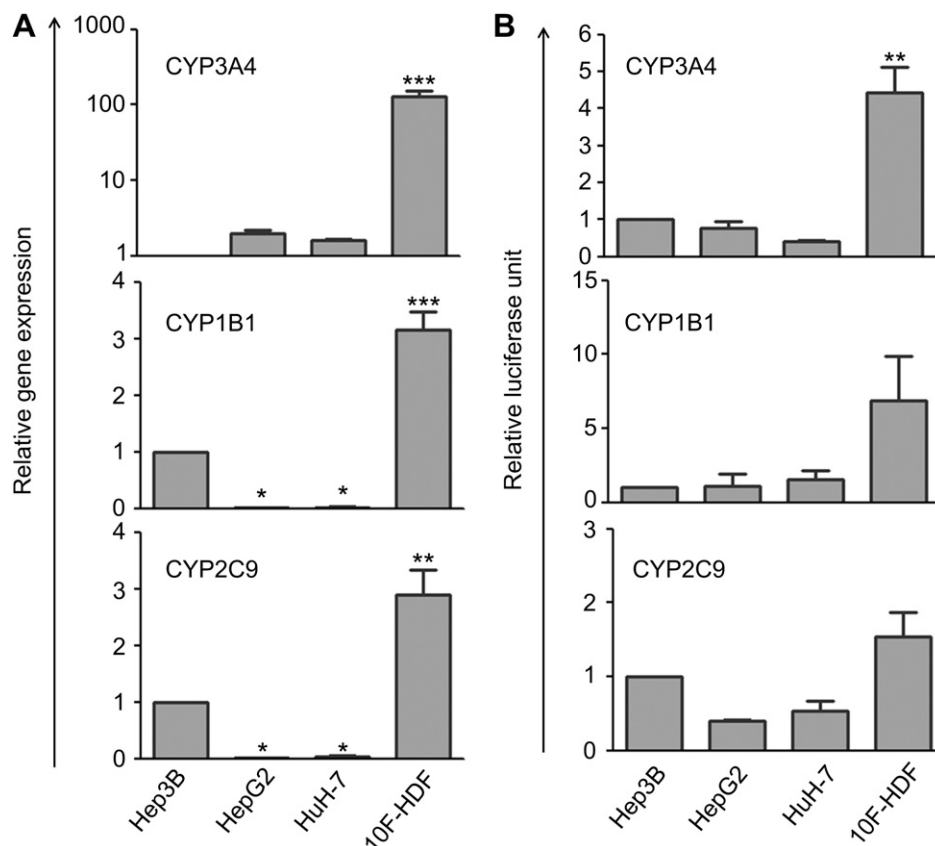


**Fig. 2.** Comparisons of 10F-HDF with 3 hepatoma cell lines Hep3B, HepG2 and HuH-7 regarding their expression levels (A) and enzyme activities (B) of CYP3A4, CYP1B1 and CYP2C9. Cells were cultured for 14 days and mRNA levels were quantified by Q-PCR. The CYP activities were presented as detected luciferase levels and normalized to respective genomic DNA amount. \**P* < 0.05, \*\**P* < 0.01, \*\*\**P* < 0.001.

activities of certain phase I enzymes CYP3A4, CYP1B1 and CYP2C9. As usual, gene expression level determined by Q-PCR was normalized to their respective house-keeping gene GAPDH. For normalizing CYP activities, the yielded luminescence levels were divided by respective genomic DNA amount.

Fig. 2 shows remarkably higher levels of the expression (Fig. 2A) and activities (Fig. 2B) of the 3 CYPs in 10F-HDFs compared to the 3 hepatoma cell lines. Using Hep3B as the standard, 10F-HDFs were 103.9-fold higher on the expression and 4.4-fold higher on the functional activity of CYP3A4. The expression and activities of CYP 1B1 were 3.1- and 6.9-fold, and of CYP2C9 2.9- and 1.5-fold higher, respectively.

### 3.3. Determination of optimal culture conditions for spheroid formation of 10F-HDFs

Cells cultured into spheroids or into 3D scaffolds have been frequently reported to enhance or maintain longer their functions or phenotypes [22,23,27,28]. Here we likewise tried to elucidate

whether 10F-HDFs cultured into spheroids and accommodated in certain scaffolds may enhance their CYP expression and activities.

First, we must decide how big the spheroids to be used. Using HydroCell dishes to form spheroids, the diameters of the formed spheroids were found closely correlated with the initial cell seeding densities. Fig. 3A shows the morphology of the spheroids formed on HydroCell dishes 4 days after culture of 10F-HDFs. The spheroids apparently became larger and larger as the initial cell seeding densities increased. After 4 days' culture, the average spheroid diameters were 35.3, 37.5, 63.8, 103.2, 163.5, and 606.7  $\mu\text{m}$ , respectively, when cells were initially seeded at densities of  $1 \times 10^5$ ,  $2 \times 10^5$ ,  $5 \times 10^5$ ,  $1 \times 10^6$ ,  $2 \times 10^6$ , and  $5 \times 10^6$  cells per 6-cm dish (surface area = 21.5  $\text{cm}^2$ ), respectively (Fig. 3B). Second, we determined the dead cell rates in the variable-sized spheroids. For this determination, we acquired the serial fluorescence images by the confocal microscopy of individual spheroids from their top to the bottom and selected the images at their largest diameter for measuring dead cell rates. Representative fluorescence images of LIVE/DEAD and Hoechst/DEAD of spheroids larger or smaller than

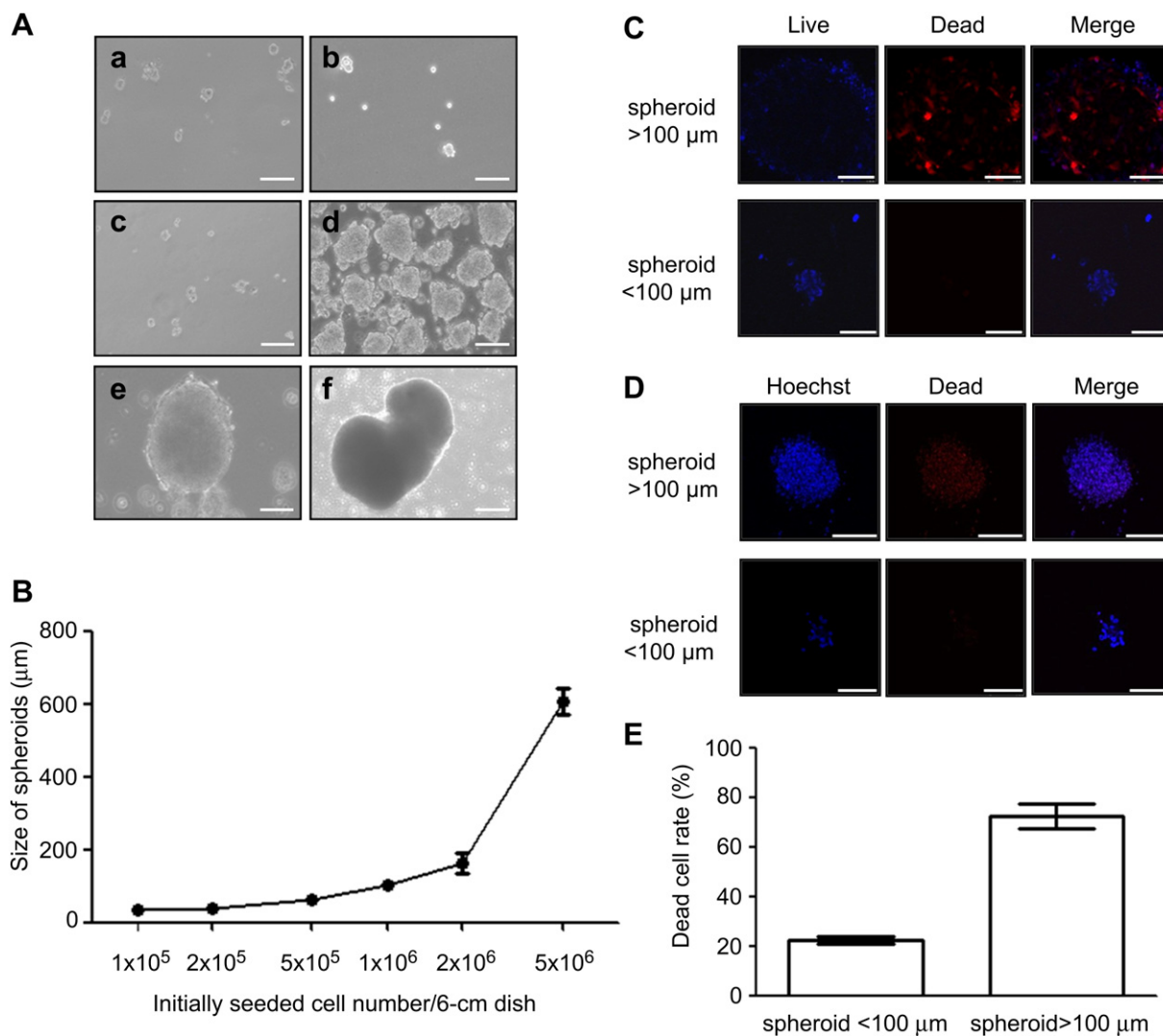


**Fig. 3.** Characterization of spheroids of 10F-HDFs formed on HydroCell dishes. (A) Representative photomicrographs showing the spheroids of 10F-HDFs initially seeded on HydroCell dishes at the densities of  $1 \times 10^5$ ,  $2 \times 10^5$ ,  $5 \times 10^5$ ,  $1 \times 10^6$ ,  $2 \times 10^6$ , and  $5 \times 10^6$  cells/6-cm dish (surface area = 21.5  $\text{cm}^2$ ). (B) The spheroid size increased as the initial cell seeding density increased. Representative fluorescence photomicrographs of LIVE/DEAD staining (C) and Hoechst/DEAD staining (D) of 10F-HDFs as spheroids at size >100  $\mu\text{m}$  (upper panel) and size < 100  $\mu\text{m}$  (lower panel) are shown. (E) Quantitative analysis of dead cell rate (number of red dead cells stained by Aqua-fluorescent reactive dye/number of total cells stained by Hoechst 34580  $\times 100\%$ ) of spheroids smaller or larger than 100  $\mu\text{m}$ . Scale bars: Aa–Ae = 100  $\mu\text{m}$ ; Af = 200  $\mu\text{m}$ ; C = 100  $\mu\text{m}$ ; D (upper panel) = 250  $\mu\text{m}$ ; D (lower panel) = 100  $\mu\text{m}$ .

100  $\mu\text{m}$  are shown in Fig. 3C and D, respectively. There was remarkably high dead cell rate (72%) in the spheroids larger than 100  $\mu\text{m}$ , while much lower rate (22%) in those smaller than 100  $\mu\text{m}$  (Fig. 3E). To minimize cell death possibly occurred in the spheroids during culturing, we therefore seeded 10F-HDFs on the 6-cm HydroCell dishes at a starting density of  $1 \times 10^6$  cells/dish in the following experiments. The spheroids thus formed had an average diameter of approximately 100  $\mu\text{m}$  after 4 days of culture.

### 3.4. Enhancement of CYP3A4 expression in 10F-HDFs cultured in various kinds of scaffolds

10F-HDFs in single cell suspension were seeded into various kinds of scaffolds and cultured for 10 days to examine which scaffold would enhance the expression of CYP3A4 in 10F-HDFs to the utmost. Compared to 10F-HDFs cultured in monolayer, expression levels of CYP3A4 in 10F-HDFs increased to 40-fold, 26-fold, 24-fold or 37-fold when the cells were cultured in gelatin, type I collagen, type IV collagen or keratin scaffold, respectively (Fig. 4). More strikingly, the expression increased to as high as 242-fold (Fig. 4) to 360-fold (Fig. 5A) when 10F-HDFs were cultured in GCH tri-copolymer scaffold. Thus GCH scaffold was chosen for further experiments.

### 3.5. Further enhancement of the gene expression and enzyme activities of CYPs in 10F-HDFs cultured as spheroids and seeded inside the GCH tri-copolymer scaffold

Next, we examined whether spheroid culture of 10F-HDFs in GCH tri-copolymer scaffold could further enhance the expression and activities of CYPs including CYP3A4. To compare with 10F-HDFs cultured in monolayer, the cells in single suspension were directly seeded into GCH scaffold (single-scaffold), cultured into spheroids on HydroCell dishes (spheroid), or the formed spheroids were further seeded and cultured in the GCH scaffolds (spheroid-

scaffold) for 1 week before determination of gene expression and enzyme activities.

Similarly to Fig. 4, Fig. 5A shows remarkable enhancement of CYP3A4 expression in single-scaffold culture (360-fold). This culture condition could not increase the expression of CYP1B1 but slightly increased the expression of CYP2C9 to 3.7-fold. Spheroid culture also markedly increased the expression of CYP3A4 (260-fold), but only slightly increased the expression of CYP1B1 (2.7-fold) and CYP2C9 (2.3-fold). Furthermore, spheroid-scaffold culture condition more significantly increased the expression of CYP3A4 to 9760-fold. Expression of CYP1B1 and CYP2C9 were increased to 7.4- and 4.6-fold, respectively.

The enzyme activities which were normalized to respective genomic DNA amount were shown in Fig. 5B. Spheroid-scaffold culture again more significantly increased the activities of the 3 CYPs (CYP3A4, 5.2-fold; CYP1B1, 2.7-fold; CYP2C9, 3.3-fold). Single-scaffold culture slightly increased the activities of CYP3A4 (3-fold), CYP1B1 (2.0-fold) and CYP2C9 (2.3-fold). Spheroid culture only mildly increased the activities of CYP3A4 (2.6-fold) but did not influence the activities of CYP1B1 (1.1-fold) and CYP2C9 (1.5-fold). Addition of rifampicin (inducer of CYP3A and CYP2C) to the spheroid-scaffold culture obviously induced enzyme activities of CYP3A4 (2.3-fold) and CYP2C9 (1.8-fold). However, omeprazole (inducer of CYP1B1) did not induce CYP1B1 activities in the spheroid-scaffold culture.

### 3.6. Demonstration of 10F-HDF spheroids accommodated within the GCH tri-copolymer scaffold

An empty scaffold imaged by SEM was shown in Fig. 6A. The pores were highly interconnected as a network which is important for cell infiltration and nutrient transportation. HDFs (Fig. 6B) and 10F-HDFs (Fig. 6C) seeded as single cell suspension in the scaffold demonstrated remarkable difference in cell morphology. The HDFs were typically fibroblastic with elongated cytoplasmic extensions, while 10F-HDFs were more or less tightly packed and with much less extensions. Fig. 6D shows irregularly shaped spheroids lodged inside the pores of the scaffold.

As there is reporter copGFP expressed by the recombinant lentiviruses, the virus-infected 10F-HDFs were readily detectable by the confocal microscopy and shown green. Fig. 6E shows cells in spheroids, small cell clusters, and as single cells inside the scaffold. A representative optical section of reconstructed microscopic images (Fig. 6F) showed scattered distribution of the spheroids and small cell clusters along the vertical plane. The larger sized spheroids tended to be lodged in the upper part of the scaffold as they were seeded by gravity in this case.

### 3.7. Persistence of enhanced CYP3A4 expression and activities in the spheroid-scaffold cultures for 2 weeks

We cultured the spheroid-scaffold constructs for 1–4 weeks to follow up their duration of enhanced CYP3A4 expression and activities. By HPLC–ESI–MS/MS, the CYP3A4 activities were here determined by measuring the amount of ONIF after incubating the constructs for 24 h with 10  $\mu\text{g}/\text{mL}$  NIF. The amount of ONIF was then normalized to respective genomic DNA amount. Fig. 7A shows CYP3A4 expression determined by Q-PCR was dramatically decreased at 3 weeks, while its activities (Fig. 7B) was highest at 1 week, and started to decline significantly since 3 weeks.

## 4. Discussion

In this study, we demonstrated the effectiveness of selected 10 hepatic transcription factors and nuclear receptors on inducing CYP

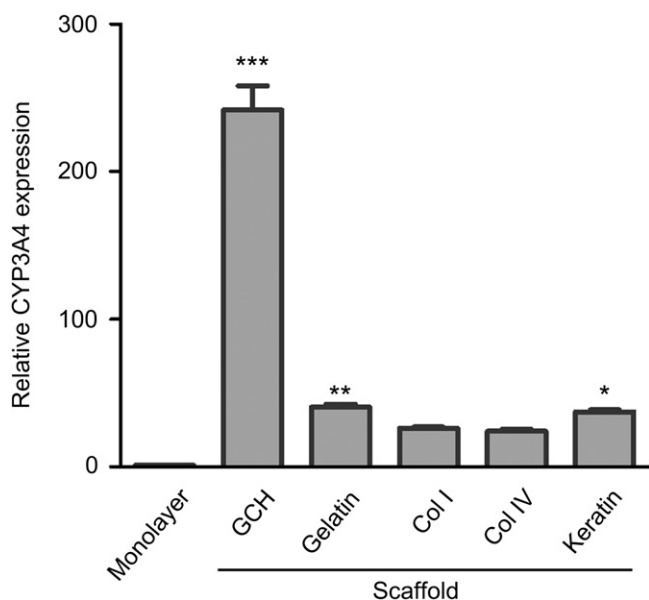


**Fig. 4.** Enhancement of CYP3A4 expression in 10F-HDFs cultured in various kinds of scaffolds. Single cell suspension was seeded by gravity into the scaffolds. Monolayer = cells cultured on polystyrene dishes as monolayer; GCH = gelatin–chondroitin–hyaluronan tri-copolymer scaffold; Gelatin = gelatin scaffold; Col I = Type I collagen scaffold; Col IV = Type IV collagen scaffold; Keratin = keratin scaffold. The expression levels were determined by Q-PCR. \* $P < 0.05$ , \*\* $P < 0.01$ , \*\*\* $P < 0.001$ .

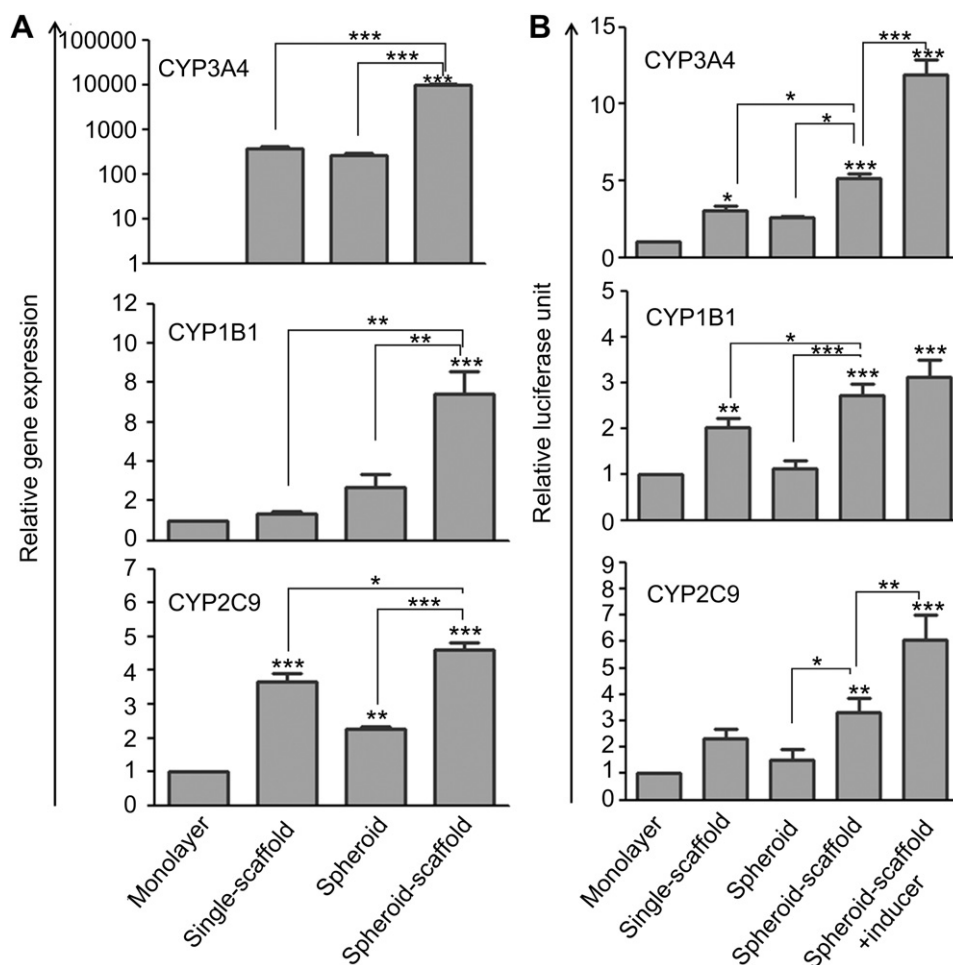


**Fig. 5.** Enhancement of CYP gene expression (A) and enzyme activities (B) of 10F-HDFs in 3D cultures. Monolayer = cells cultured on polystyrene dishes as monolayer; Single-scaffold = single cell suspension cultured in GCH tri-copolymer scaffold; Spheroid = cells cultured on HydroCell dishes to form spheroids; Spheroid-scaffold = spheroids formed for 4 days and then cultured in GCH scaffolds for 7 days. The expression levels were determined by Q-PCR. The CYP activities in B were presented as detected luciferase levels normalized to respective genomic DNA amount. Inducers rifampicin (for CYP3A4 and CYP2C9) and omeprazole (for CYP1B1) were added to show their inducing activities of these CYP enzymes. \* $P < 0.05$ , \*\* $P < 0.01$ , \*\*\* $P < 0.001$ .

expression and activities in HDFs. Moreover, we showed these induced expression and activities might be further enhanced as the cells were formed into spheroids and accommodated in GCH tri-copolymer scaffold.

CYPs are major phase I enzymes playing central roles in the metabolism and detoxification of various endogenous and exogenous compounds introduced into the body [12]. CYP3A4 is abundant in the human liver and metabolize more than 50% of clinically used drugs [12,14]. Therefore, in this study we used CYP3A4 as the primary end to select factors in combination mostly enhancing its expression. It has been shown that liver-enriched transcription factors and nuclear receptors regulate expression of most CYPs at transcriptional level [13,15,17,18,31]. HNF1 (composed of HNF1 $\alpha$  and HNF1 $\beta$  hetero- or homodimers), HNF4 $\alpha$ , and HNF6 are important regulators in controlling liver development and also appear to be involved in the control of liver-specific expression of several CYP genes [31]. A significant down-regulation of CYP3A4 gene has been shown in cultured human hepatocytes transfected with HNF4 $\alpha$  antisense RNA, indicating that HNF4 $\alpha$  is an important factor controlling expression of CYP3A4 in hepatocytes [31,32]. PXR, an orphan nuclear receptor, has been implicated a predominant regulator of CYP3A subfamily in response to the exposure of various xenobiotics [33–35]. Keeping in line, our data shown in Fig. 1A and B also demonstrated a most dramatic reduction of the expression of

CYP3A4 when PXR was removed from the pool of delivered factors, suggesting PXR was the most important factor. Although the effect of GR on the regulation of CYP3A was still in debate, a dose-dependent experiment has been shown that dexamethasone, a GR ligand, has positive effect on CYP3A4 induction [36]. In addition, GR was shown to have a synergistic effect with PXR in regulating CYP3A4 expression [15,36]. To our surprise, our approach has excluded RXR that has been frequently implicated to form heterodimer with PXR to activate the expression of CYP3A4 [15]. Other CYPs, such as CYP1B1, are regulated by a heterodimer composed of AhR and its nuclear translocator (ARNT) [37–39]. The results shown in Fig. 1B indicated that HNF4 $\alpha$ , HNF6, PXR, GATA6, and HLX1 were the major regulators for CYP3A4 as removal of anyone from the pool resulted in a remarkable reduction of the expression. Among them, PXR appeared to be the master regulator. Using our strategy by omitting respective ones from the total pool of 24 factors, we finally selected 10 factors (Fig. 1A and B). More strikingly is that delivery of total 24 factors only increased very little the expression of CYP3A4, while delivery of only the 10 selected factors dramatically increased the expression to 120,000-fold (Fig. 1C). These results suggested some of the factors finally excluded might have strong down-regulatory effects, and showed our approach was successful in obtaining an optimal pool of factors: HNF1 $\alpha$ , HNF1 $\beta$ , HNF4 $\alpha$ , HNF6, ARNT, PXR, GATA6, GP130R, GR and HLX1.

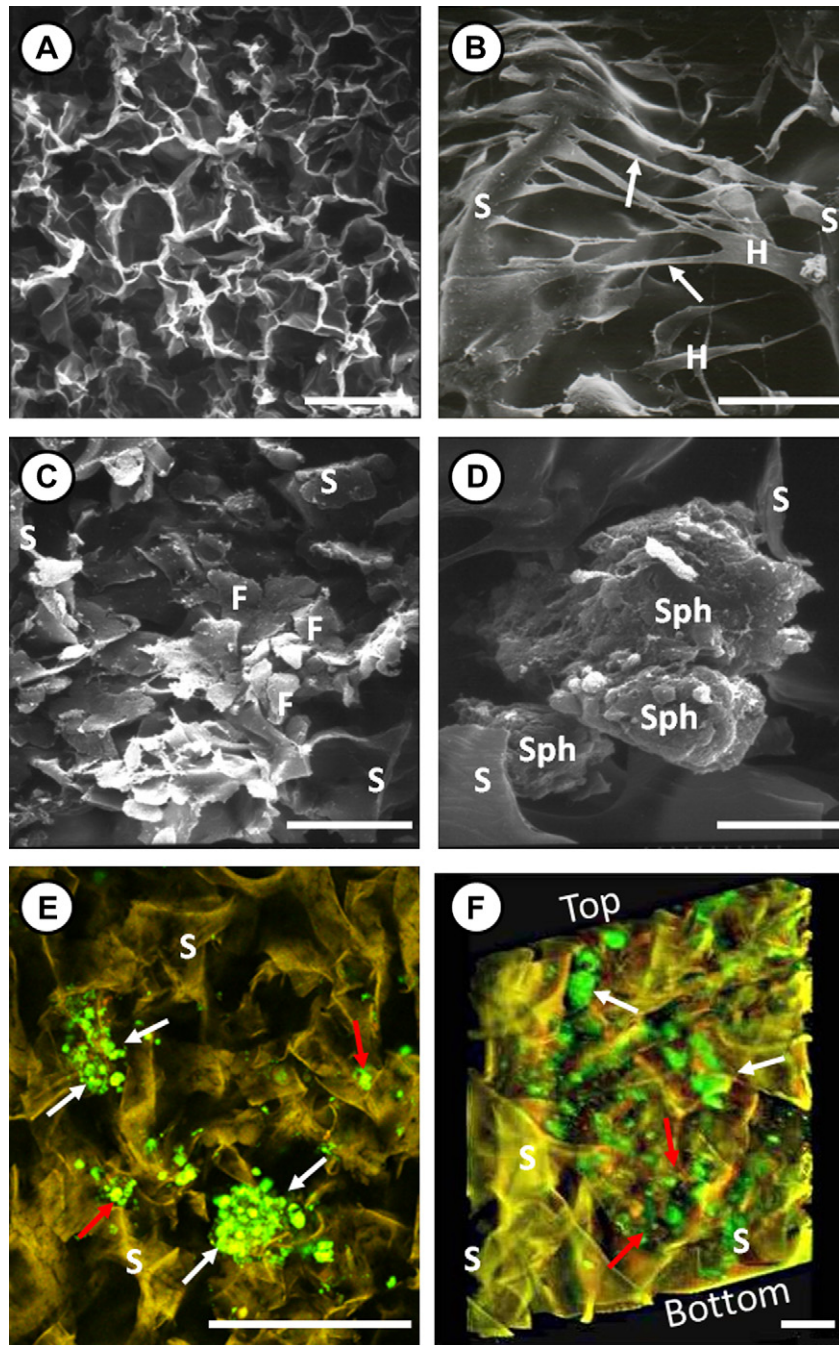


**Fig. 6.** Images of SEM (A–D) and confocal microscopy (E–F) of tri-copolymer scaffolds seeded with 10F-HDFs. (A) The morphology of GCH tri-copolymer scaffold. Single cell-seeded HDFs (B) and 10F-HDFs (C) on scaffolds after 14 days of culture demonstrated different cell morphology. HDFs were with long extensions, while 10F-HDFs were more compact and not extended. Arrows indicate fibroblastic extensions. (D) Spheroids of 10F-HDFs grown in the pores of the scaffold are clearly shown. (E) 10F-HDFs with reporter copGFP fluorescence are shown in a scaffold. White arrows indicate spheroids and red arrows indicate cells in small clusters or single. (F) An optic section from top to the bottom of the reconstructed confocal microscopic images in E. White arrows indicate spheroids and red arrows indicate cells in small clusters or single. The spheroids tended to be lodged on the upper portion of the scaffold. H = HDFs; F = 10F-HDFs; S = scaffold; Sph = spheroid. Scale bars: A = 200  $\mu\text{m}$ ; B and C = 60  $\mu\text{m}$ ; D = 43  $\mu\text{m}$ ; E = 100  $\mu\text{m}$ ; F = 25  $\mu\text{m}$ .

Drug-induced hepatotoxicity is a big health threat possibly leading to acute liver failure and may cause drug withdrawals from the market [1–3]. Because human hepatoma cell lines are easily obtainable, they were frequently used for drug toxicity testing. Unfortunately, one major drawback of these cells is their very low expression of CYPs, limiting their usefulness as a reliable test [8,40,41]. The activities of most CYPs were undetectable in these hepatoma cells lines by functional assays, and only very sensitive techniques like Q-PCR could detect the expression of the CYP genes.

The much higher activity levels of many CYPs in 10F-HDFs in our study indicated that these cells would be more suitable than those commonly used hepatoma cell lines for drug toxicity testing. Compared to Hep3B, 10F-HDFs were 4.4-fold, 6.9-fold and 1.5-fold higher in the activities CYP3A4, CYP1B1 and CYP2C9, respectively (Fig. 2B).

Maintenance of cellular functions is not only controlled by autonomous intracellular programs but also influenced by cell–cell and cell–matrix interactions [19]. Many approaches have been

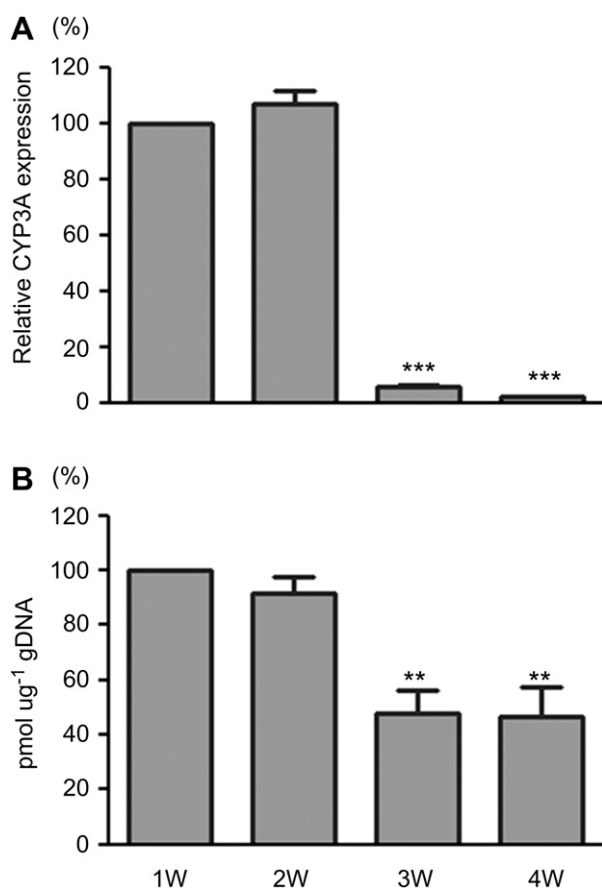


**Fig. 7.** The expression level (A) and enzyme activities (B) of CYP3A4 by the spheroid-scaffold constructs of 10F-HDFs cultured for 1–4 weeks. The gene expression levels of CYP3A4 were determined by Q-PCR. The metabolism activities of CYP3A4 by the spheroid-scaffold constructs were determined by measuring metabolized oxidized nifedipine from nifedipine that is a substrate of CYP3A4. Oxidized nifedipine was quantified by HPLC–ESI–MS/MS. W = week. \* $P < 0.05$ , \*\* $P < 0.01$ , \*\*\* $P < 0.001$ .

used to maintain the functions of human hepatocytes *in vitro*, including optimization of culture medium [42], culturing on extracellular matrix [43], using co-culture system [44] and construction of 3D microenvironment [45]. 3D culture systems have been implicated in improving cell–cell and cell–matrix interactions and maintaining cellular functions [20–22]. The benefits of enhancing gene expression and sustaining cell functions have been frequently demonstrated in a variety of 3D culture systems such as culturing cells in natural or synthetic scaffolds or as spheroids [46]. Primary hepatocytes cultured into spheroids had higher viability and functions than those cultured under traditional monolayer culture system [26]. The scaffolds could provide support for cell attachment, migration, growth and mass transport. This present study demonstrated GCH tri-copolymer scaffold was the best among the tested scaffolds to enhance CYP3A4 expression in 10F-HDFs seeded as single cell suspension (Fig. 4). Spheroid culture also significantly increased the expression of CYP3A4 and CYP2C9 (Fig. 5A). Moreover, combining spheroid formation and seeding the spheroids into GCH tri-copolymer scaffolds further enhanced the expression and activities of the 3 CYPs (Fig. 5). The orders of the increment in the expression and functional activities of CYP3A4 were not in parallel and were much higher in the former than in the latter (Figs. 2 and 7). This indicated a low regression coefficient or a discordant expression between mRNA and protein. The discordant expression is commonly seen [47–49] and may be caused by post-transcriptional regulations such as micro-RNAs [50].

Spheroid formation is a commonly used 3D culture method. However, previous methods to form spheroids were difficult to control their size [23]. The size of the spheroids is of critical importance because the core of the spheroids can easily undergo necrosis due to inadequate inward permeation of nutrients and oxygen when the spheroids are larger than 150  $\mu\text{m}$  [51]. Hence, it is better to check cell viability in spheroids of different size and use spheroids in uniform size for application. We found in this study the mean size of spheroids formed on HydroCell dishes were positively correlated with the initial cell seeding densities (Fig. 3A and B). Furthermore, our data showed only 22% of cells in the spheroids smaller than 100  $\mu\text{m}$  are dead, in contrast to as high as 72% dead cell rate in spheroids larger than 100  $\mu\text{m}$  (Fig. 3E). We thus chose an optimal cell seeding density to yield spheroids smaller than 100  $\mu\text{m}$  for further studies.

In this study, we used two inducers to induce CYP activities. Rifampicin was shown actively induce the enzyme activities of CYP3A4 and CYP2C9, while omeprazole failed to induce CYP1B1 activity (Fig. 5B). Rifampicin is a ligand inducer able to bind and activate PXR [52] that had been exogenously expressed by lentivirus transduction in 10F-HDFs. Its addition not surprisingly induced activities of CYP3A4 and CYP2C9 whose expression was mainly regulated by PXR. In contrast, omeprazole induces the activity of CYP1B1 through binding AhR [53]. Because AhR was not included in the 10-factor induction system of this study, omeprazole could not induce the CYP1B1 activity (Fig. 5B).

To validate the potential of using 10F-HDF spheroid-scaffold constructs in drug metabolism tests, we chose nifedipine, a clinically used antihypertensive drug metabolized by CYP3A4, as a substrate to test the drug metabolism activity [54,55]. The data demonstrated that these constructs maintained their CYP3A4 gene expression and drug metabolism activity for 2 weeks (Fig. 7). It is longer than human primarily cultured hepatocytes whose such activity can only persist for 1–2 days after *in vitro* culturing [10,11]. The expression and activities of CYP3A4 decreased abruptly and dramatically since 3 weeks of culture (Fig. 7). The reason was unclear.

The expression of drug-metabolizing enzymes, mainly CYPs and phase II enzymes, in the liver shows significant inter-species and inter-individual variations making accurate prediction of specific drug's potential of hepatotoxicity in human individuals difficult if the testing is based on animal hepatocytes or limited sources of human hepatocytes [56,57]. Genetic polymorphism of various CYPs and phase II enzymes is an important cause for inter-individual variations in drug toxicity potential [58]. In this study, we chose human dermal fibroblasts that can be more easily obtained and rapidly propagated *in vitro* than primary hepatocytes. If the fibroblasts can be collected from people with various genetic backgrounds, drug toxicity testing based on a number of cell sources may partly overcome the problem of genetic polymorphism-related inter-individual variations leading to failure of detecting drug toxicity if the tests are based on cells from single or a few origins.

## 5. Conclusion

HDFs exogenously delivered with 10 selected factors expressed much higher levels of phase I enzyme CYP3A4, CYP2C9 and CYP1B1 than 3 commonly used hepatoma cell lines HepG2, Hep3B and HuH-7. Furthermore, culturing of these cells into spheroids and seeding them into GCH tri-copolymer scaffolds collectively further augmented these phase I enzyme activities. This approach demonstrated the superiority of the scaffold culture to the conventional monolayer culture, and may have potential to be used as a valuable testing system for drug metabolism and toxicity.

## Conflict of interest

The authors confirm that there are no conflicts of interest.

## Acknowledgments

This work was supported by grants from National Science Council (NSC99-3114-B-002-006 to G.T.H) and National Taiwan University Hospital (VN100-05 to H.S.L). Flow cytometry and HPLC–ESI–MS/MS was performed at the Joint Center for Instruments and Researches, College of Bioresources and Agriculture, National Taiwan University, Taiwan.

## References

- [1] Chang CW, Beland FA, Hines WM, Fuscoe JC, Han T, Chen JJ. Identification and categorization of liver toxicity markers induced by a related pair of drugs. *Int J Mol Sci* 2011;12:4609–24.
- [2] Kaplowitz N. Idiosyncratic drug hepatotoxicity. *Nat Rev Drug Discov* 2005;4:489–99.
- [3] Schuster D, Laggner C, Langer T. Why drugs fail—a study on side effects in new chemical entities. *Curr Pharm Des* 2005;11:3545–9.
- [4] MacDonald JS, Robertson RT. Toxicity testing in the 21st century: a view from the pharmaceutical industry. *Toxicol Sci* 2009;110:40–6.
- [5] Pritchard JF, Jurima-Romet M, Reimer ML, Mortimer E, Rolfe B, Cayen MN. Making better drugs: Decision gates in non-clinical drug development. *Nat Rev Drug Discov* 2003;2:542–53.
- [6] Committee on Toxicity Testing and Assessment of Environment Agents, National Research Council. Toxicity testing in the 21st century: a vision and a strategy. <http://www.nap.edu/catalog/11970.html.Toxicity>; 2007.
- [7] Guillouzo A. Liver cell models in in vitro toxicology. *Environ Health Perspect* 1998;106(Suppl. 2):511–32.
- [8] Brandon EF, Raap CD, Meijerman I, Beijnen JH, Schellens JH. An update on in vitro test methods in human hepatic drug biotransformation research: pros and cons. *Toxicol Appl Pharmacol* 2003;189:233–46.
- [9] Wilkening S, Stahl F, Bader A. Comparison of primary human hepatocytes and hepatoma cell line HepG2 with regard to their biotransformation properties. *Drug Metab Dispos* 2003;31:1035–42.
- [10] Sivaraman A, Leach JK, Townsend S, Iida T, Hogan BJ, Stolz DB, et al. A microscale in vitro physiological model of the liver: predictive screens for drug metabolism and enzyme induction. *Curr Drug Metab* 2005;6:569–91.
- [11] Hewitt NJ, Lechon MJ, Houston JB, Halifax D, Brown HS, Maurel P, et al. Primary hepatocytes: current understanding of the regulation of metabolic enzymes and transporter proteins, and pharmaceutical practice for the use of hepatocytes in metabolism, enzyme induction, transporter, clearance, and hepatotoxicity studies. *Drug Metab Rev* 2007;39:159–234.
- [12] Guengerich FP. Cytochrome p450 and chemical toxicology. *Chem Res Toxicol* 2008;21:70–83.
- [13] Xu C, Li CY, Kong AN. Induction of phase I, II and III drug metabolism/transport by xenobiotics. *Arch Pharm Res* 2005;28:249–68.
- [14] Tarantino G, Di Minno MN, Capone D. Drug-induced liver injury: is it somehow foreseeable? *World J Gastroenterol* 2009;15:2817–33.
- [15] Wang H, LeCluyse EL. Role of orphan nuclear receptors in the regulation of drug-metabolising enzymes. *Clin Pharmacokinet* 2003;42:1331–57.
- [16] Lee TI, Young RA. Transcription of eukaryotic protein-coding genes. *Annu Rev Genet* 2000;34:77–137.
- [17] Odom DT, Zizlsperger N, Gordon DB, Bell GW, Rinaldi NJ, Murray HL, et al. Control of pancreas and liver gene expression by HNF transcription factors. *Science* 2004;303:1378–81.
- [18] Honkakoski P, Negishi M. Regulation of cytochrome P450 (CYP) genes by nuclear receptors. *Biochem J* 2000;347:321–37.
- [19] Khetani SR, Bhatia SN. Microscale culture of human liver cells for drug development. *Nat Biotechnol* 2008;26:120–6.
- [20] Griffith LG, Swartz MA. Capturing complex 3D tissue physiology in vitro. *Nat Rev Mol Cell Biol* 2006;7:211–24.
- [21] Abu-Absi SF, Friend JR, Hansen LK, Hu WS. Structural polarity and functional bile canaliculi in rat hepatocyte spheroids. *Exp Cell Res* 2002;274:56–67.
- [22] Lu HF, Chua KN, Zhang PC, Lim WS, Ramakrishna S, Leong KW, et al. Three-dimensional co-culture of rat hepatocyte spheroids and NIH/3T3 fibroblasts enhances hepatocyte functional maintenance. *Acta Biomater* 2005;1:399–410.
- [23] Sakai Y, Yamagami S, Nakazawa K. Comparative analysis of gene expression in rat liver tissue and monolayer- and spheroid-cultured hepatocytes. *Cells Tissues Organs* 2010;191:281–8.
- [24] Khalil M, Shariat-Panahi A, Tootle R, Ryder T, McCloskey P, Roberts E, et al. Human hepatocyte cell lines proliferating as cohesive spheroid colonies in alginate markedly upregulate both synthetic and detoxificatory liver function. *J Hepatol* 2001;34:68–77.
- [25] Du Y, Han R, Ng S, Ni J, Sun W, Wohland T, et al. Identification and characterization of a novel prespheroid 3-dimensional hepatocyte monolayer on galactosylated substratum. *Tissue Eng* 2007;13:1455–68.
- [26] Chia SM, Leong KW, Li J, Xu X, Zeng K, Er PN, et al. Hepatocyte encapsulation for enhanced cellular functions. *Tissue Eng* 2000 Oct;6:481–95.
- [27] Yin C, Mien Chia S, Hoon Quek C, Yu H, Zhuo RX, Leong KW, et al. Microcapsules with improved mechanical stability for hepatocyte culture. *Biomaterials* 2003;24:1771–80.
- [28] Moghe PV, Berthiaume F, Ezzell RM, Toner M, Tompkins RG, Yarmush ML. Culture matrix configuration and composition in the maintenance of hepatocyte polarity and function. *Biomaterials* 1996;17(3):373–85.
- [29] Chang CH, Liu HC, Lin CC, Chou CH, Lin FH. Gelatin-chondroitin-hyaluronan tri-copolymer scaffold for cartilage tissue engineering. *Biomaterials* 2003;24:4853–8.
- [30] Kuo TF, Lin HC, Yang KC, Lin FH, Chen MH, Wu CC, et al. Bone marrow combined with dental bud cells promotes tooth regeneration in miniature pig model. *Artif Organs* 2011;35:113–21.
- [31] Akiyama TE, Gonzalez FJ. Regulation of P450 genes by liver-enriched transcription factors and nuclear receptors. *Biochim Biophys Acta* 2003;1619:223–34.
- [32] Jover R, Bort R, Gomez-Lechon MJ, Castell JV. Cytochrome P450 regulation by hepatocyte nuclear factor 4 in human hepatocytes: a study using adenovirus-mediated antisense targeting. *Hepatology* 2001;33:668–75.
- [33] Moore LB, Goodwin B, Jones SA, Wisely GB, Serabjit-Singh CJ, Willson TM, et al. St. John's wort induces hepatic drug metabolism through activation of the pregnane X receptor. *Proc Natl Acad Sci U S A* 2000;97:7500–2.
- [34] Coumoul X, Diry M, Barouki R. PXR-dependent induction of human CYP3A4 gene expression by organochlorine pesticides. *Biochem Pharmacol* 2002;64:1513–9.
- [35] Moore JT, Kliever SA. Use of the nuclear receptor PXR to predict drug interactions. *Toxicology* 2000;153:1–10.
- [36] Pascucci JM, Drocourt L, Gerbal-Chaloin S, Fabre JM, Maurel P, Vilarem MJ. Dual effect of dexamethasone on CYP3A4 gene expression in human hepatocytes. Sequential role of glucocorticoid receptor and pregnane X receptor. *Eur J Biochem* 2001;268:6346–58.
- [37] Kawajiri K, Fujii-Kuriyama Y. Cytochrome P450 gene regulation and physiological functions mediated by the aryl hydrocarbon receptor. *Arch Biochem Biophys* 2007;464:207–12.
- [38] Hankinson O. The aryl hydrocarbon receptor complex. *Annu Rev Pharmacol Toxicol* 1995;35:307–40.
- [39] Fujii-Kuriyama Y, Mimura J. Molecular mechanisms of AhR functions in the regulation of cytochrome P450 genes. *Biochem Biophys Res Commun* 2005;338:311–7.
- [40] Guo L, Dial S, Shi L, Branham W, Liu J, Fang JL, et al. Similarities and differences in the expression of drug-metabolizing enzymes between human hepatic cell lines and primary human hepatocytes. *Drug Metab Dispos* 2010;39:528–38.
- [41] Hewitt NJ, Hewitt P. Phase I and II enzyme characterization of two sources of HepG2 cell lines. *Xenobiotica* 2004;34:243–56.
- [42] Mizumoto H, Ishihara K, Nakazawa K, Ijima H, Funatsu K, Kajiwara T. A new culture technique for hepatocyte organoid formation and long-term maintenance of liver-specific functions. *Tissue Eng Part C Methods* 2008;14:167–75.
- [43] Bissell DM, Arenson DM, Maher JJ, Roll FJ. Support of cultured hepatocytes by a laminin-rich gel. Evidence for a functionally significant subendothelial matrix in normal rat liver. *J Clin Invest* 1987;79:801–12.
- [44] Thomas RJ, Bhandari R, Barrett DA, Bennett AJ, Fry JR, Powe D, et al. The effect of three-dimensional co-culture of hepatocytes and hepatic stellate cells on key hepatocyte functions in vitro. *Cells Tissues Organs* 2005;181:67–79.
- [45] Tong JZ, De Lagausie P, Furlan V, Cresteil T, Bernard O, Alvarez F. Long-term culture of adult rat hepatocyte spheroids. *Exp Cell Res* 1992;200:326–32.
- [46] Hammond JS, Beckingham IJ, Shakesheff KM. Scaffolds for liver tissue engineering. *Expert Rev Med Devices* 2006;3:21–7.
- [47] Chen G, Gharib TG, Huang CC, Taylor JM, Misk DE, Kardias SL, et al. Discordant protein and mRNA expression in lung adenocarcinomas. *Mol Cell Proteomics* 2002;1:304–13.
- [48] Guo Y, Xiao P, Lei S, Deng F, Xiao GG, Liu Y, et al. How is mRNA expression predictive for protein expression? A correlation study on human circulating monocytes. *Acta Biochim Biophys Sin (Shanghai)* 2008;40:426–36.
- [49] Ghazalpour A, Bennett B, Petyuk VA, Orozco L, Hagopian R, Mungro IN, et al. Comparative analysis of proteome and transcriptome variation in mouse. *PLoS Genet* 2011;7:e1001393.
- [50] Takagi S, Nakajima M, Mohri T, Yokoi T. Post-transcriptional regulation of human pregnane X receptor by micro-RNA affects the expression of cytochrome P450 3A4. *J Biol Chem* 2008;283:9674–80.
- [51] Funatsu K, Ijima H, Nakazawa K, Yamashita Y, Shimada M, Sugimachi K. Hybrid artificial liver using hepatocyte organoid culture. *Artif Organs* 2001;25:194–200.
- [52] Chen J, Raymond K. Roles of rifampicin in drug–drug interactions: underlying molecular mechanisms involving the nuclear pregnane X receptor. *Ann Clin Microbiol Antimicrob* 2006;5:3.
- [53] Tompkins LM, Wallace AD. Mechanisms of cytochrome P450 induction. *J Biochem Mol Toxicol* 2007;21:176–81.
- [54] Haas DM, Quinney SK, McCormick CL, Jones DR, Renbarger JL. A pilot study of the impact of genotype on nifedipine pharmacokinetics when used as a tocolytic. *J Matern Fetal Neonatal Med* 2011;–5. Early Online.
- [55] Patki KC, Von Moltke LL, Greenblatt DJ. In vitro metabolism of midazolam, triazolam, nifedipine, and testosterone by human liver microsomes and

- recombinant cytochromes p450: role of cyp3a4 and cyp3a5. *Drug Metab Dispos* 2003;31:938–44.
- [56] Daly AK, Aithal GP, Leathart JB, Swainsbury RA, Dang TS, Day CP. Genetic susceptibility to diclofenac-induced hepatotoxicity: contribution of UGT2B7, CYP2C8, and ABCC2 genotypes. *Gastroenterology* 2007;132:272–81.
- [57] Huang YS, Chern HD, Su WJ, Wu JC, Chang SC, Chiang CH, et al. Cytochrome P450 2E1 genotype and the susceptibility to antituberculosis drug-induced hepatitis. *Hepatology* 2003;37:924–30.
- [58] Chalasani N, Bjornsson E. Risk factors for idiosyncratic drug-induced liver injury. *Gastroenterology* 2010;138:2246–59.